SUPPLEMENTARY METHODS

Animals: *Slc9a3* null knockout mice ($NHE3^{-/-}$) and their wild-type littermates ($NHE3^{+/+}$) were bred on the original mixed genetic background (129/Black Swiss) whereas *Slc9a2* knockout mice ($NHE2^{-/-}$) as well as wild-type littermates ($NHE2^{+/+}$) were bred on the original Non-Swiss Albino background. Mice were bred and maintained in a conventional animal facility at the University of Arizona. Water and food were provided *ad libitum*. Breeders (heterozygous) were maintained on Teklad Global 2019 (19% protein extruded) diet, and experimental mice on NIH-31 Modified Open Formula Mouse/Rat Diet (7013; both from Harlan Teklad, Madison, WI). At weaning, mice were genotyped by PCR using genomic DNA from tail biopsy as described[19]. Genotyping of *Slc9a2* knockout mice was done using forward (CATCTCTATCACAAGTTGCCCACAATCGTG) and reverse (GTGACTGCATCGTTGAGCAGAGACTCG) primers corresponding to sequences from near the 5' and 3' ends of the second exon and a primer from near the 3' end of the neomycin resistance gene (GACAATAGCAGGCATGCTGG) to amplify 450- and 221-base pair (bp) products from the wild-type and mutant genes, respectively [32]. Sentinel mice were routinely monitored and determined as free from common murine pathogens (MHV, MPV, MVM, TMEV, Mycoplasma pulmonis, Sendai, EDIM, MNV, ecto- and endoparasites). All mice were obtained as a kind gift from Dr. Gary E. Shull. 6-8 week old knockout mice or their genetically matched wild-type (WT) littermates mice were left untreated or given drinking water with increasing concentration (0.5-4%) of DSS for up to 7 days. In a separate series of experiments, mice received drinking water supplemented with broad spectrum antibiotics (ciprofloxacin, 200 mg/l; metronidazole, 500 mg/l) for 10 days prior to sacrifice or DSS administration[19], or received two injections (in 48 hr interval) of rabbit IgG or anti-Asialo GM1 antibodies (Wako, Richmond,

VA; 100 μg/mouse). All animal protocols and procedures were approved by the University of Arizona Animal Care and Use Committee.

Tissue collection: Mice were euthanized by CO_2 inhalation followed by cervical dislocation. Small intestines and colons were then dissected and flushed with PBS. Tissues for histological studies and in-situ hybridization (ISH) staining were immediately fixed in 10% buffered formalin (Fisher Scientific, Pittsburgh, PA), dehydrated with increasing concentrations of ethanol and xylene, and embedded in paraffin. Tissue fragments for immunohistochemical staining on frozen sections were embedded in Tissue-Tek (O.C.T., Sakura Finetek, Inc. Torrance, CA), frozen in liquid nitrogen and stored at -80°C until analysis. All samples were cut into 5μm-thick sections. Tissues for gene expression analyses were frozen immediately in liquid nitrogen, stored at -80°C until their use for subsequent RNA extraction and then analyzed by either microarray or real-time PCR techniques. Blood samples for hematology analysis were collected into tubes with EDTA (BD Microtainer tubes, Becton Dickinson, NJ) by cardiac puncture.

Isolation of intraepithelial and lamina propria lymphocytes, magnetic sorting and flow cytometry: IEL and LPL cells were isolated from the small intestine from NHE3$^{-/-}$ mice and their wild-type littermates according to a previously described method[33] with minor modifications. Briefly, after removing Peyer's patches the intestines were cut into 1-2 cm sections, everted and washed in DMEM containing 5% FBS. Due to differences in cell yield, sections from two WT mice were combined, whereas NHE3$^{-/-}$ mice were processed individually. The sections were placed into the medium with 5% FBS, 1mM EDTA and 1mM DTT, and incubated for 20 min at 37°C. Samples were shaken vigorously for 1 min and IEL were

collected. Tissues were transferred to the DMEM medium with 5% FBS and 50 U/ml of collagenase (Sigma) and incubated at 37°C for 1.5 hours with gentle shaking. Medium was changed twice every 45 min. Collected cells were washed in medium with 5% FBS and IEL and LPL populations were further fractionated by centrifugation (2500 x g, 20 min, at room temp) in a 40%/70% Percoll gradient. Cells were collected from the interphase. Cells were counted and their viability was estimated by the trypan blue exclusion method. IEL and LPL populations were tested for IFN-γ expression by real-time RT-PCR as described below. For flow cytometry, LPL ($1x10^6$) were washed in PBS and were first incubated with an Fc receptor-blocking Ab (1:50; BD Pharmingen) for 5 min at 4°C, then cells were incubated for 30 min with saturating amounts of the selected anti-mouse antibodies. For single and/or double staining FITC-conjugated CD8α, CD3ε, CD11c (eBiosciences), PerCP-conjugated CD3ε (BD Pharmingen), FITC-conjugated TCRα (Beckman Coulter) were used. Cells stained for Asialo-GM1 were incubated with rabbit anti-ASGM1 Ab (Wako, Japan) followed by secondary anti-rabbit IgG conjugated with Alexa 647 (Invitrogen). Negative isotype controls were used for each staining. Cells were analyzed using a FACScalibur (Becton Dickinson Immunocytometry Systems). A minimum of 10,000 events was collected for each sample, and data analysis was performed with the CellQuest software (Becton Dickinson). In a separate series of experiments, LPL cells were magnetically sorted using CD8α or CD4 beads into $CD8^+$ and $CD4^+$ populations according to the manufactures instructions (Miltenyi Biotec, Bergisch Gladbach, Germany). After selection, cells were washed and resuspended in complete medium (RPMI 1640, Invitrogen) supplemented with 10% heat-inactivated fetal calf serum (Gemini Bio-Products, West Sacramento, CA), 2 mM L-glutamine, and penicillin (100 U/ml)-streptomycin (100 μg/ml) (Invitrogen). Then, $CD4^+$ or $CD8^+$ T cells were stimulated with 50ng/ml of PMA (Sigma), 1μg/ml ionomycin (Sigma) in the

presence of 1μl/ml of GolgiPlug™ (Brefeldin A- BD Bioscience), for 6 hours at 37°C in a 5% CO_2 atmosphere. After a wash in 1X PBS, cells were incubated with Fc receptor-blocking antibodies (BD pharmingen, San Jose, CA) for 5 min at 4°C. Then FITC-conjugated anti-CD4 (rat IgG2b, BD pharmingen) or PerCP-conjugated anti-CD8 (rat IgG2a, BD Pharmingen) antibodies were incubated for 30 minutes at the dilution 1:50 in 1X PBS at 4°C. Then, cells were washed in 1X PBS and fixed in 1% paraformaldehyde/0.5% saponin/1%BSA for 20 minutes at 4°C. After washing in 0.5% saponin/1%BSA/1X PBS, cells were stained with the PE-conjugated IFNγ antibodies (rat IgG1, BD pharmingen) diluted 1:50 in 0.5% saponin/1%BSA/1X PBS. After washes, cells were resuspended in 1X PBS and analyzed using FACScalibur (Becton Dickinson).

Hematology: Hematology profile analyses with full differential were done by an experienced pathologist at the University Animal Care Pathology Services, the University of Arizona using the Hemavet 850 Mascot (Drew Scientific, Farmington, CT).

Real-time RT-PCR: Expression of selected genes was independently analyzed by real-time RT-PCR. Total RNA (200ng) was reverse-transcribed (RT) using the qScript cDNA Synthesis Kit (Quanta Biosciences Inc, Gaithersburg, MD), and 2μl of each RT reaction (10% of total volume of real-time reaction mixture) was used for real-time PCR analysis using TaqMan technology and commercially available primers (Mm00801778_m1 for IFN-γ, Mm00440485_m1 for NOS2 and Mm00438656_m1 for ET-1; Mm00516703_s1 for claudin 2; all from Applied Biosystems (Foster City, CA)), PerfeCTa qPCR SuperMix (Quanta Biosciences Inc, Gaithersburg, MD) and the iCycler optical PCR cycler (Bio-Rad). Resulting data were analyzed by the comparative

cycle threshold (Ct) method as means of relative quantitation of gene expression, normalized to an endogenous reference (TATA-box binding protein, TBP) and relative to a calibrator (normalized Ct value obtained from control mice) and expressed as 2Ct (Applied Biosystems User Bulletin no. 2: Rev B "Relative Quantitation of Gene Expression").

Western blot analysis*:* Previously collected small intestinal tissues were homogenized in RIPA buffer (0.1% SDS, 1% Na-deoxycholate in TBS) with protease and phosphatase inhibitors (Pierce, Rockford, IL), clarified by centrifugation and protein level in each sample was determined (BCA Protein Assay, Pierce). 50µg of tissue extracts were loaded onto 8% polyacrylamide gels (Invitrogen) in Laemmli sample buffer. Gels were blotted on 0.45 µm nitrocellulose membranes (Fisher Scientific). Membranes were labeled with monoclonal anti-mouse phospho-Stat1 (pY701, Cell Signaling Technology, Danvers, MA) or with polyclonal (E-23) anti-mouse total Stat1 (Santa Cruz Biotechnology) followed by peroxidase-conjugated anti-rabbit IgG (Amersham–GE Healthcare, UK) and chemiluminescence detection with SuperSignal West Pico reagent (Pierce). Glyceraldehyde 3-phosphate dehydrogenase (GAPDH) was used as a loading control. Phosphorylation status of Stat1 was expressed as ratio of pY701/total Stat1.

Immunohistochemistry and transmission electron microscopy (TEM): For occluding and E-cadherin staining, sections (5 µm) were cut and transferred onto glass slides and fixed 10 min in cold methanol. Slides were incubated for 30 min in PBS supplemented with serum corresponding to the secondary antibody isotype and 1% BSA. Next, sections were incubated with the appropriate dilution of anti-occludin, or anti-E-cadherin primary antibodies (both from Zymed/Invitrogen) for 1 hour at room temperature. Secondary detection was performed with

antibodies conjugated to Alexa-647 (Molecular Probes, Invitrogen). Slides were counterstained with Sytox-Green to visualize nuclei (Molecular Probes). Images were acquired using a Bio-Rad MRC1024ES laser scanning confocal microscope at 600x magnification. Sections from four mice of respective genotypes were analyzed and representative images presented. F-actin was stained with Alexa-647-conjugated phalloidin (Molecular Probes), counterstained and images were acquired as previously described. For ApopTag assay, cleaved caspase-3 and Ki67, 5μm tissue-sections were mounted on Med frost slides. After deparaffinization and rehydratation, antigen retrieval was performed by heating slides in 1X citrate buffer (Dako, Carpinteria, CA). After washing in H_2O, residual endogenous peroxidase activity was quenched by incubation in 3% H_2O_2 in water for 10 min. Slides were then blocked with 5% normal goat serum (Vector Laboratories, Burlingame, CA) for 1 hour in 1X TBS/0.1% Tween-20 (TBST) or 1X PBS/0.1% BSA, for cleaved caspase-3 and Ki67, respectively. Next, sections were incubated with the primary antibody against cleaved-caspase 3 (Cell Signaling Technology, Danvers, MA; 1:100 dilution in TBST/5% normal goat serum) or against Ki67 (Thermo Scientific, Fremont, CA; 1:200 dilution in 1X PBS/1% BSA) overnight at 4°C. After 3 washes in TBST or 1X PBS, slides were incubated with biotinylated secondary antibody and streptavidin/peroxidase complex according to the manufacturer's recommendation (Vector Laboratories). Slides were then incubated with 3-amino-9-ethylcarbazole, AEC (Vector laboratories) and mounted with Dakomounting medium (Dako North America, Inc. Carpinteria, CA). Slide examination was performed independently by 2 experienced scientists in a blind manner using a Zeiss Axioplan microscope (Carl Zeiss MicroImaging, Thornwood, NY), images were captured with Nikon Digital Sight DS-Fi1 camera and NIS-Element software (Nikon Instruments, Melville, NY). Staining was scored by counting the number of cleaved caspase-3 positive cells per high-power

field (200x magnification) as blinded samples. A total of five fields in randomly chosen sections were analyzed for each group.

For ApopTag *in situ* oligo ligation (ISOL) apoptosis detection the sections were prepared as described above. After deparaffinization and rehydratation slides were pretreated with Proteinase K (Fisher Scientific, 50µg/ml in PBS). Further steps were done according to manuafcturer's instructions and slides were mounted with mounting medium (Dako). Images were captured as described above.

For TEM, samples were fixed in half-strength Karnovsky's in 0.1M cacodylate buffer, post-fixed in 2% osmium tetroxide, rinsed in 0.1M cacodylate buffer and dehydrated in a graded series of ethanols. Samples were then embedded in Spurr resin. Thin sections (60-90 nm) were cut and placed on 150 mesh copper grids and stained with uranyl acetate and lead citrate. The grids were examined on a Philips CM-12 microscope at 80kV. Images were recorded on Kodak 4489 electron image film and scanned for documentation.

In-situ hybridization (ISH): Tissue sections were deparaffinized, treated with proteinase K (MBI, Rockville, MD), dehydrated, and dried at room temperature. For detection of IFN-γ transcript, we used the Ultra-sensitive In situ Hybridization Detection Kit with specific biotinylated DNA probes (both from MBI) according to the manufacturer's protocol. Slides were then mounted with a permanent mounting medium (Vector laboratories, Burlingame, CA) and the images were captured with the Zeiss Axioplan microscope (Carl Zeiss MicroImaging, Thornwood, NY), fitted with Nikon Digital Sight DS-Fi1 camera at 400 x magnification and NIS-Element software (Nikon Instruments, Melville, NY).

Histological evaluation: Sections of the proximal and/or distal colon were deparaffinized and rehydrated by use of standard procedures. For histological analysis, standard hematoxylin and eosin (H&E) staining was performed and digitally documented as described for ISH. NIS-Element software (Nikon Instruments), was used for morphometric analysis of villi length and crypt depths.

Intestinal permeability: Transmucosal tracer flux was analyzed using two different markers: dextran labeled with fluorescein isothiocyanate (FITC) (average M.W. 4,000) and FITC-labeled 5-(and-6)-sulfonic acid, trisodium salt (M.W. 478.32). Prepared solutions in PBS were administrated by gastric gavage at the final dose of 60mg /100g B.W. and 20mg /100g B.W., respectively, to WT or $NHE3^{-/-}$ mice treated with water or 4% DSS 48 hours before the gavage. After 4 hours mice were euthanized by CO_2 anesthesia followed by cervical dislocation. Blood samples were collected on heparin by cardiac puncture and the resulting plasma was assayed for fluorescence in 96-well black plates using Ascent FL Fluoroscan plate reader (excitation: 485nm; emission: 527nm) and calculated against a respective standard curve. Results were expressed as a molar concentration of FITC-labeled markers in the blood.

Nitric oxide determination: To determine the ileal NO content, we utilized the Nitric Oxide Quantitation Kit (Active Motif, Carlsbad, CA) based on nitrate and nitrite determination after enzymatic conversion. Tissues were homogenized in the assay buffer (250µl of buffer per 100mg of tissue) provided with the kit. All debris were removed by centrifugation (21,000 x g, 40 min, 4°C) and supernatant was transferred into centrifugal filters (Centricon Ultracel YM-10, 10kDa cut-off, Millipore) and centrifuged (6,500 x g, 65 min, 4°C) to remove high molecular weight

proteins that can interfere with the nitrate reductase and/or Griess reaction as recommended by the manufacturer. To maintain pH of the samples, which was affected by the alkaline content obtained from $NHE3^{-/-}$ mice, samples were diluted 2 times in the assay buffer.

Microarray analysis of colonic gene expression: Mucosal scrapings from the entire small intestine or colon (except 2 cm of rectum) were obtained from 18 $NHE3^{-/-}$ mice (9 control, 9 treated with 4% DSS for 48 hrs) and from 18 analogously treated wilt-type littermates. Samples were pooled (three mice per sample) and RNA was purified with RNeasy Midi Kit (Qiagen) to yield three samples per genotype per treatment. RNA integrity was evaluated with Agilent 2100 BioAnalyzer microfluidics-based platform (Agilent, Foster City, CA). RNA samples were subsequently processed as described [19] to yield biotinylated cRNA for hybridization to Affymetrix GeneChip Mouse Genome 430 2.0 arrays (Affymetrix, Santa Clara, CA). The GeneChip Mouse Genome 430 2.0 array is a single array comprised of over 45,000 probe sets representing over 34,000 well-substantiated mouse genes. Stringent empirical and statistical analyses were employed to compare gene expression profiles between wild-type and $NHE3^{-/-}$ mice with cross-gene error model based on replicates. Normalized data (per gene, per chip, and per sample with healthy controls serving as a reference point) were serially filtered in the following order: eliminate genes flagged as absent in all groups, select genes up- or down-regulated at least two-fold with $P \leq 0.05$ (wild-type vs. NHE3/ mice, Student t-test with Benjamini and Hochberg false discovery rate as multiple testing correction).

SUPPLEMENTARY FIGURE LEGENDS

Suppl. Figure 1. Real-time PCR analysis of the changes in expression of IFN-γ (**A**), iNOS (**B**) , and endothelin 1 (**C**; ET-1) in the small intestine and colon of NHE3-deficient mice. Gene expression was normalized to TATA box–binding protein as an internal control using the ΔΔCt method, with expression values in WT mice used as a calibrator. (**D**) Analysis of NO concentration in the ileal contents of WT and $NHE3^{-/-}$ mice. Asterisks indicate significant differences between WT and $NHE3^{-/-}$ mice (T-test, $p<0.05$).

Suppl. Figure 2. *Expression and activation of Stat1 in the small intestinal mucosa of $NHE3^{-/-}$ mice*. (**A**) Representative Western blot of pY701-Stat1, total Stat1, and GAPDH. (**B**) Summary of results of total Stat1 expression (Stat1:GAPDH ratio) and (**C**) Stat1 activation (pY701-Stat1:total Stat1 ratio). Asterisks indicate significant differences between WT and $NHE3^{-/-}$ mice (T-test, $p<0.05$; n=4)

Suppl. Figure 3. **(A)** Cleaved caspase-3 immunostaining in the small intestinal mucosa of WT and $NHE3^{-/-}$ mice. Arrows point to typical apoptotic cells stained with the red chromogen (3-amino-9-ethylcarbazole). (**B**) Graph summary of caspase-3 positive cell count per field of vision calculated in a blinded fashion. No statistically significant differences were observed.

Suppl. Figure 4. *Ki67 staining of proliferating cells in the the small intestinal mucosa of WT and NHE3$^{-/-}$ mice.* With the exception of increased number of Ki67-positive mononuclear cells infiltrating the lamina propria, no significant differences were observed for the epithelial cells.

Suppl. Figure 5. **(A)** Histogram depicting the number of genes/probe sets which expression was increased or reduced at $P<0.05$ in NHE3$^{-/-}$ mice relative to their wild-type littermates (Student t-test with Benjamini and Hochberg false discovery rate as multiple testing correction). Increasing stringency of analysis (2-10 fold change on X-axis) demonstrates the magnitude of change in small intestinal gene expression profile in NHE3$^{-/-}$ mice. **(B)** Gene ontology analysis using DAVID Functional Annotation Tool (http://david.abcc.ncifcrf.gov/) of the 1,256 non-duplicated and well annotated genes which indicated >2-fold change at $p<0.05$ (Student t-test with Benjamini and Hochberg false discovery rate as multiple testing correction). Genes categorized based on biological process were grouped and ranked (threshold of 5, $P<0.05$). Categories were sorted according to the EASE score, a modified Fisher exact P value.

Supplemental Table 1. Selection of genes related to the immune and inflammatory response with expression altered ≥2-fold ($p \leq 0.05$) in the small intestinal mucosa of $NHE3^{-/-}$ mice. Genes were grouped in respective ontologic category based on the analysis with Functional Annotation Tool and the Database Annotation, Visualization, and Integrated Discovery (DAVID; http://david.abcc.ncifcrf.gov) developed and maintained by the National Institute of Allergy and Infectious Diseases (22), as described in the Materials and Methods section. Within categories, genes are sorted according to the magnitude of response.

	Gene Symbol	Gene Bank Accession	Gene name	Fold change
Antigen Presentation	Ifnγ	K00083	interferon gamma	5.70
	H2-Q7	M29881	histocompatibility 2, Q region locus 7	4.73
	H2-DMβ1	NM_010387	histocompatibility 2, class II, locus Mβ1	4.54
	H2-Aβ1	NM_010379	histocompatibility 2, class II antigen A, beta 1	4.29
	H2-Q8	AK013097	histocompatibility 2, Q region locus 8	4.02
	H2-Aα	BE688749	histocompatibility 2, class II antigen A, alpha	3.29
	H2-DMα	NM_010386	histocompatibility 2, class II, locus DMα	3.29
	H2-Q1	BC010602	histocompatibility 2, Q region locus 1	3.17
	Cd74	BC003476	CD74 antigen	2.60
	H2-T23	NM_010398	histocompatibility 2, T region locus 23	2.42
	Psmb9	NM_013585	proteasome (prosome, macropain) subunit, beta type 9	2.38
	H2-D1	NM_010380	histocompatibility 2, D region locus 1	2.27
	H2-Eb1	NM_010382	histocompatibility 2, class II antigen E beta	2.25
	Tapbp	AF043943	TAP binding protein	2.24
	Ap3β1	BM222025	adaptor-related protein complex 3, beta 1 subunit	2.13
Chemotaxis	Cxcl9	NM_008599	chemokine (C-X-C motif) ligand 9	4.19
	Ccl5	NM_013653	chemokine (C-C motif) ligand 5	3.87
	Ccl28	NM_020279	chemokine (C-C motif) ligand 28	3.54
	Ccl20	AF099052	chemokine (C-C motif) ligand 20	3.51
	Ccr2	BB148128	chemokine (C-C motif) receptor 2	2.79
	Ccl4	AF128218	chemokine (C-C motif) ligand 4	2.32
	Cxcl10	NM_021274	chemokine (C-X-C motif) ligand 10	2.24
Leukocyte activation	Cd274	NM_021893	CD274 antigen	7.26
	Lat	AF036907	linker for activation of T cells	6.73
	Dclre1c	BB479896	DNA cross-link repair 1C, PSO2 homolog (S. cerevisiae)	3.71
	Dclre1c	BB479896	DNA cross-link repair 1C, PSO2 homolog (S. cerevisiae)	3.71
	Casp3	D86352	caspase 3	3.34
	Cd5	NM_007650	CD5 antigen	3.24
	Cd28	NM_007642	CD28 antigen	3.17
	Itgam	NM_008401	integrin alpha M	2.67
	Tpd52	AI427778	Tumor protein D52	2.61
	Lcp2	NM_010696	lymphocyte cytosolic protein 2	2.31
	Cd3δ	NM_013487	CD3 antigen, delta polypeptide	2.30
	Itgb2	NM_008404	integrin beta 2	2.29
	Lck	AA867167	lymphocyte protein tyrosine kinase	2.27
	Cd3γ	M58149	CD3 antigen, gamma polypeptide	2.25
	Cd8α	BB154331	CD8 antigen, alpha chain	2.21
	Cd3ε	NM_007648	CD3 antigen, epsilon polypeptide	2.16
	Ap3β1	BM222025	adaptor-related protein complex 3, beta 1 subunit	2.13
	Exo1	NM_012012	exonuclease 1	2.11
	Hsp90αa1	BG242724	heat shock protein 90, alpha (cytosolic), class A member 1	2.06
	Thy1	AV028402	thymus cell antigen 1, theta	2.04
	Tgfβr2	BG793483	transforming growth factor, beta receptor II	2.04
	Unc13d	AK011827	unc-13 homolog D (C. elegans)	2.03
	Bcl10	AF100339	B-cell leukemia/lymphoma 10	2.00
	Bcl3	NM_033601	B-cell leukemia/lymphoma 3	2.00
	Prlr	NM_008932	prolactin receptor	2.00
	Cd24α	NM_009846	CD24α antigen	0.34

Supplemental Table 1 (cont.)

	Gene Symbol	Gene Bank Accession	Gene name	Fold change
Immune response	Gbp1	NM_010259	guanylate nucleotide binding protein 1	14.10
	Gbp2	NM_010260	guanylate nucleotide binding protein 2	11.50
	Tgtp	NM_011579	T-cell specific GTPase	9.32
	Gzmb	NM_013542	granzyme B	6.73
	Mpa2l/Gbp6	NM_194336	macrophage activation 2 like, guanylate binding protein 6	6.52
	Il18bp	AF110803	interleukin 18 binding protein	6.23
	Ifit2	NM_008332	interferon-induced protein with tetratricopeptide repeats 2	5.74
	Indo	NM_008324	indoleamine-pyrrole 2,3 dioxygenase	4.31
	Oasl2	BQ033138	2'-5' oligoadenylate synthetase-like 2	3.65
	Serpina3g	BC002065	serine (or cysteine) peptidase inhibitor, clade A, member 3G	3.64
	Irf8	NM_008320	interferon regulatory factor 8	3.45
	Gzmk	AB032200	granzyme K	3.17
	Crtam	NM_019465	cytotoxic and regulatory T cell molecule	3.10
	Tap1	BC024897	transporter 1, ATP-binding cassette, sub-family B (MDR/TAP)	3.09
	Isg15	AK019326	ISG15 ubiquitin-like modifier	3.06
	Samhd1	NM_018851	SAM domain and HD domain, 1	3.05
	Ifi202b	NM_011940	interferon activated gene 202B	3.04
	Gzma	NM_010370	granzyme A	3.02
	Ctla4	NM_009843	cytotoxic T-lymphocyte-associated protein 4	2.83
	Oasl1	AB067533	2'-5' oligoadenylate synthetase-like 1	2.81
	Ly96	NM_016923	lymphocyte antigen 96	2.65
	Cfh	AI987976	complement component factor h	2.57
	Gp49a	U05264	glycoprotein 49 A	2.45
	C2	AV290571	complement component 2 (within H-2S)	2.42
	Clec4a2	BC006623	C-type lectin domain family 4, member a2	2.41
	Rnf19b	AK015966	ring finger protein 19B	2.36
	Il4ra	NM_010557	interleukin 4 receptor, alpha	2.30
	Cd7	NM_009854	CD7 antigen	2.24
	Pglyrp1	NM_009402	peptidoglycan recognition protein 1	2.18
	Clec4n	AF240358	C-type lectin domain family 4, member n	2.15
	Il1f9	AY071843	interleukin 1 family, member 9	2.04
	Igj	BC006026	immunoglobulin joining chain	2.03
	Ptms	AK011360	parathymosin	0.45
	Cd55	BM208097	CD55 antigen	0.35
	Ambp	NM_007443	alpha 1 microglobulin/bikunin	0.34
Inflammatory response (incl. acute phase)	Saa1	NM_009117	serum amyloid A 1	64.50
	Nos2	AF065921	nitric oxide synthase 2, inducible, macrophage	23.70
	Saa2	NM_011314	serum amyloid A 2	15.80
	Chst4	AK009113	carbohydrate (chondroitin 6/keratan) sulfotransferase 4	6.19
	Saa3	NM_011315	serum amyloid A 3	5.09
	Itgb6	NM_021359	integrin beta 6	4.00
	Thbs1	AI385532	thrombospondin 1	3.08
	Tac1	NM_009311	tachykinin 1	2.93
	Reg3g	NM_011260	regenerating islet-derived 3 gamma	2.58
	Cd14	NM_009841	CD14 antigen	2.46
	Tollip	BB400304	toll interacting protein	2.41
	Smad1	NM_008539	MAD homolog 1 (Drosophila)	2.28
	Nfkbiz	NM_030612	nuclear factor of kappa light polypeptide gene enhancer in B-cells inhibitor, zeta	2.18
	Ptger3	NM_011196	prostaglandin E receptor 3 (subtype EP3)	2.17
	Bmp2	AV239587	bone morphogenetic protein 2	1.99
	Ndst1	AF074926	N-deacetylase/N-sulfotransferase (heparan glucosaminyl) 1	1.67
	Alox5	BB079625	arachidonate 5-lipoxygenase	0.36

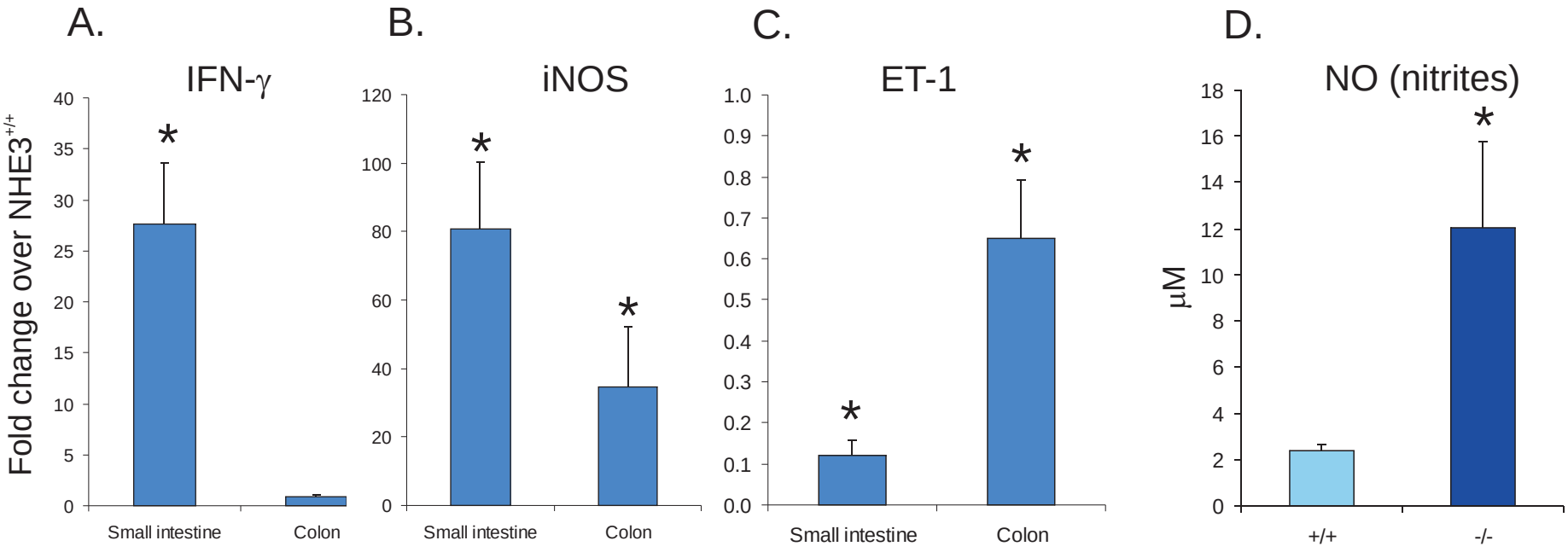

Supplement
Figure 1.

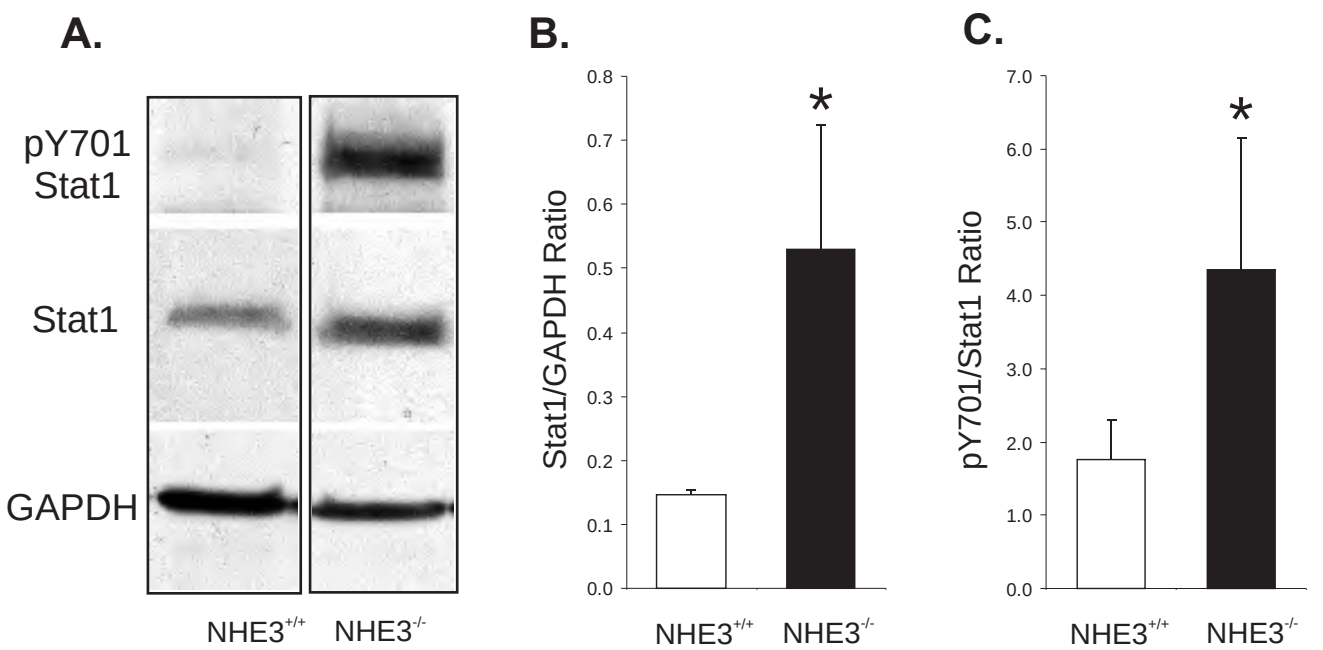

Supplement
Figure 2.

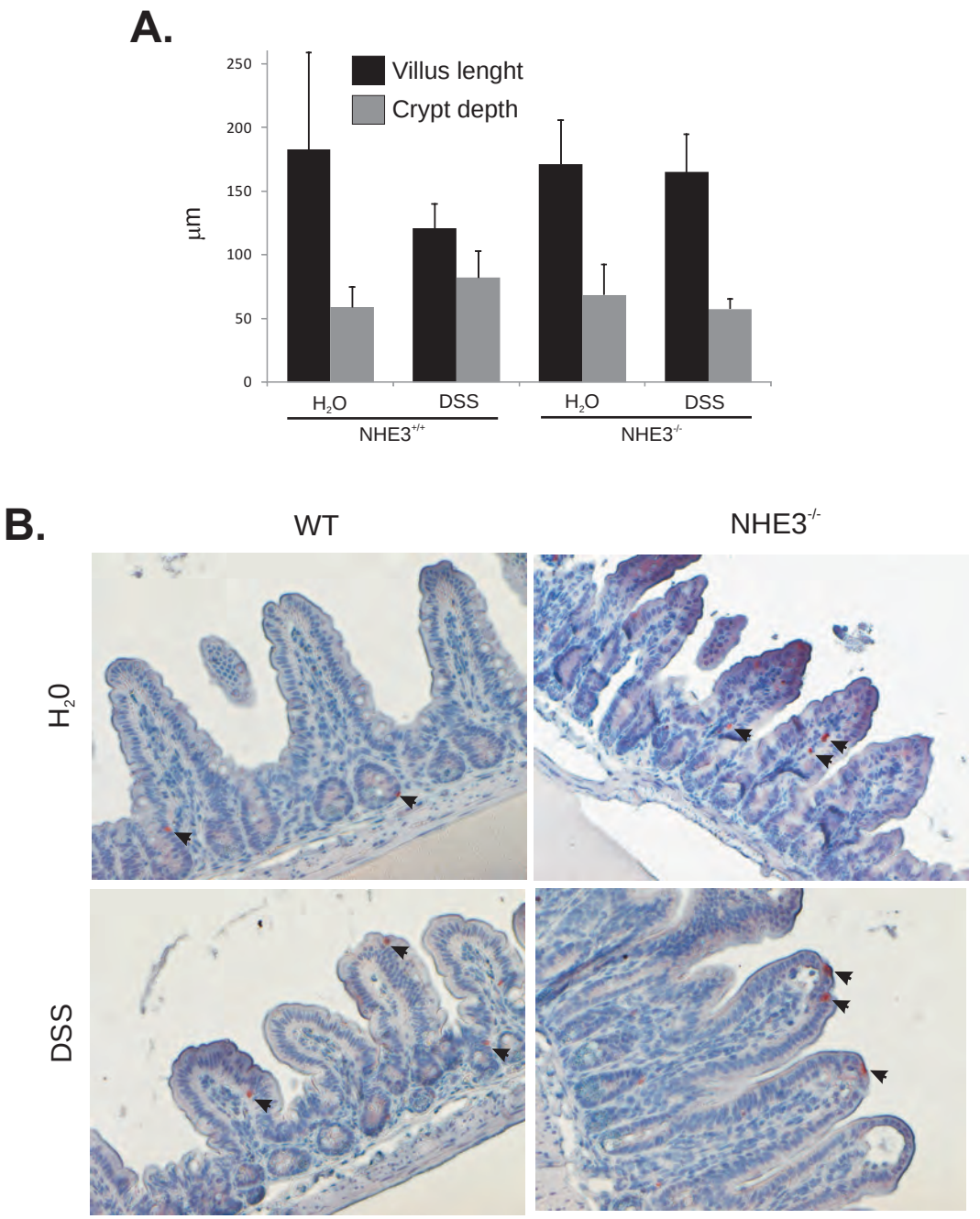

Supplement
Figure 3.

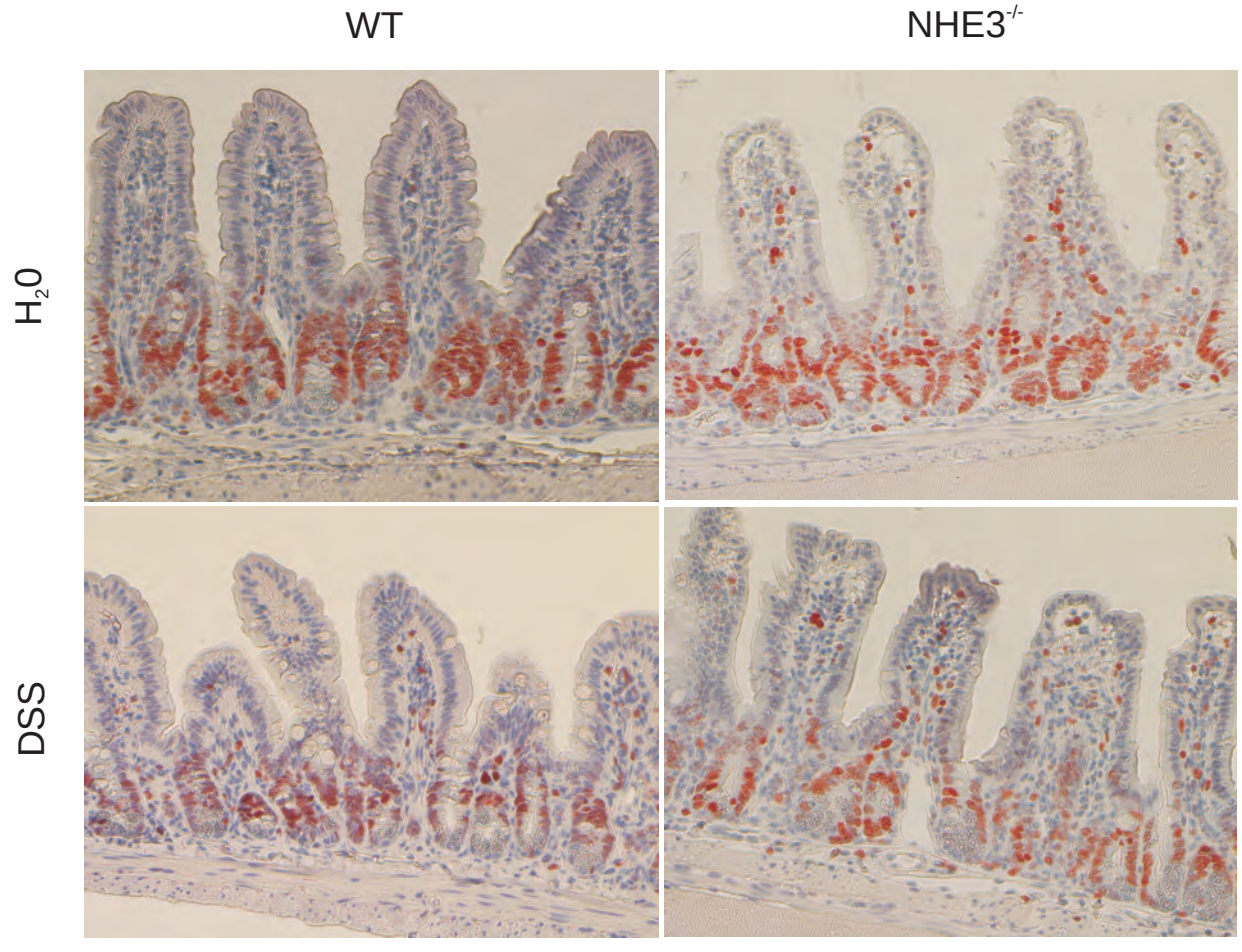

Supplement
Figure 4.

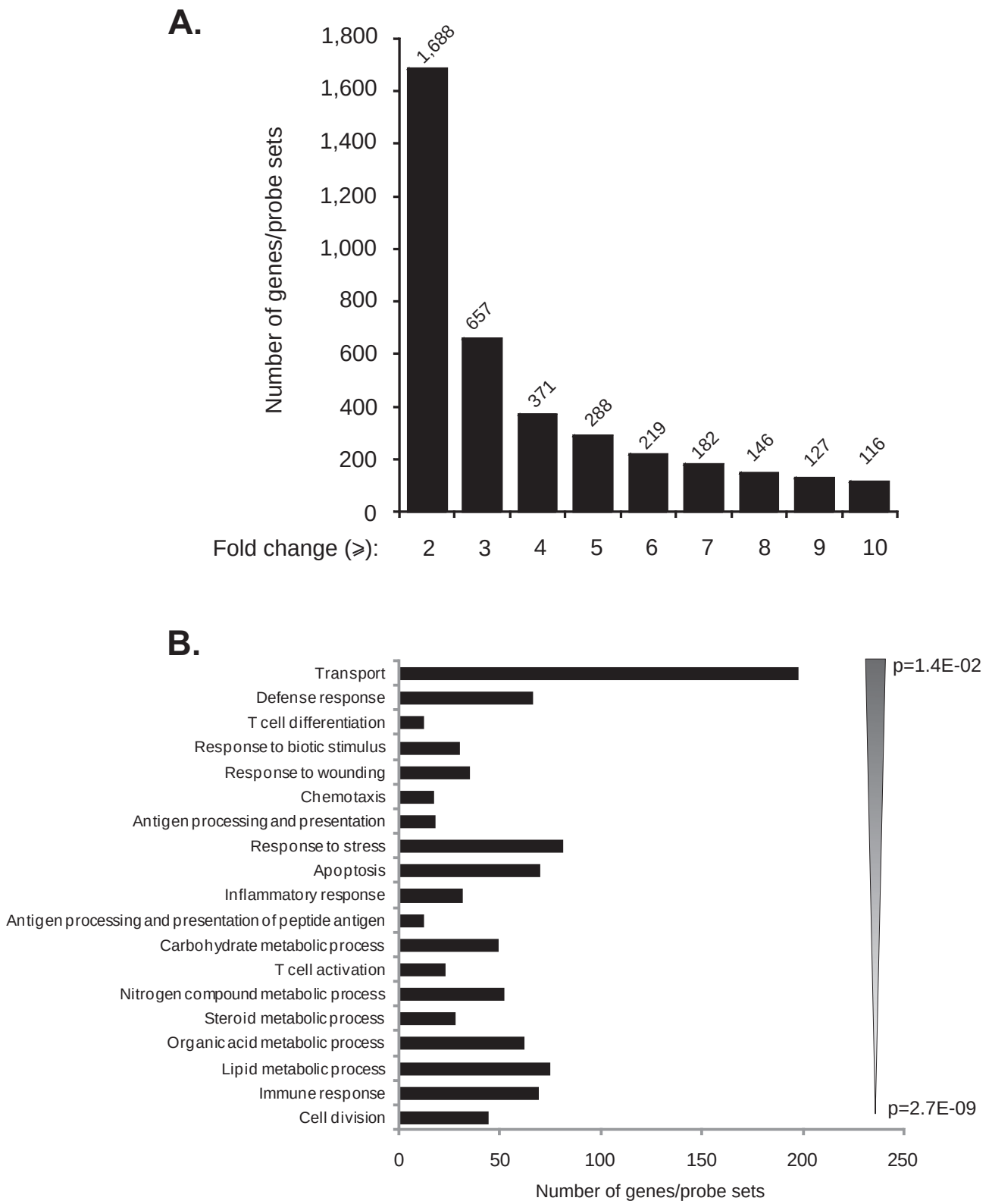

Supplement
Figure 5.